15.4 DEFINING THE LIFECYCLE OF THE EXTRATROPICAL TRANSITION OF TROPICAL CYCLONES USING THE DEVIATION ANGLE VARIANCE TECHNIQUE FOR REMOTELY-SENSED IMAGERY

David E. Kofron*, Miguel F. Piñeros, Elizabeth A. Ritchie, and J. Scott Tyo
University of Arizona, Tucson, Arizona

1. INTRODUCTION

The extratropical transition (ET) of tropical cyclones (TCs) is a process in which recurving, warm-core TCs propagate poleward and interact with mid-latitude features, such as a cold-core pre-existing extratropical cyclone or trough, and transition into mid-tropical cyclones. During ET, TCs encounter environmental changes, such as increased Coriolis, decreased SSTs, and strong westerly flow and vertical wind shear. These changes cause drastic changes in the TC structure as it becomes an extratropical cyclone, which include, but are not limited to, an increase in the gale force wind field, increase in precipitation poleward and downstream, and a decrease in the asymmetry of the TC (Jones et. al. 2003). These environmental changes often increase the translation speed of the storm and the size of the storm while decreasing the maximum wind speed. The increase in the size and speed along with increased environmental westerly vertical shear causes the decaying TC to become very asymmetric and may contribute to the generation of large waves and swells (Jones et. al. 2003). Also, many of these TCs become powerful extratropical cyclones and pose a threat to land and marine interests similar to that of TCs, whereas others may completely dissipate. The interaction between the mid-latitude features and the TC is not well understood, so it is difficult to forecast the intensity of a fully transitioned storm. Forecasting the speed and location of the transitioning TC is also problematic because small errors in the initial location of the TC can result in large errors in the 24 and 48-hour numerical weather prediction forecast. Forecast problems with speed, location, and intensity make it challenging to forecast the location of the high winds and precipitation and the oceanic response to the transitioned cyclone (Jones et. al. 2003).

The ET lifecycle can be divided into two stages – transformation and reintensification (Klein et. al. 2000). The beginning of the transformation stage, often referred to as “ET time”, begins as the TC becomes more asymmetric due to interaction with strong westerly wind shear. Once the remainder of the TC becomes embedded in the baroclinic zone, the transformation stage is ended (Klein et. al 2000). This time is called the “ET completion time”. In order to better understand and potentially improve forecasting of ET, these times must be better defined.

Several studies objectively classify the ET time and ET completion time using cyclone phase-space (Hart 2003; Evans and Hart 2002), frontogenesis (Harr and Elsberry 2001), geopotential heights (Demirci et. al. 2007), and potential vorticity (Kofron et. al. 2009b). However, these objective measures have been shown to have inconsistencies, including reliance on gridded analyses and computational difficulties (Kofron et al. 2009a and 2009b). More recently, an objective measure for examining cyclone symmetry called the deviation angle variance technique (DAV-T) has been designed for use on developing tropical cyclones using satellite infrared (IR) imagery (Piñeros et. al. 2008; 2009). The DAV-T values, while characterizing cloud structure, are found to be strongly correlated with TC intensity. Because of the distinctive changes in tropical cyclone symmetry during extratropical transition as described by Klein et al. (2000), this study attempts to define the ET lifecycle using the DAV-T.

* *Corresponding author address:* David E. Kofron, Univ. of Arizona, Dept. of Atmospheric Science, Tucson, AZ 85721-0081.
email: kofron@atmo.arizona.edu.

2. DATA & METHODS

The data used in this study are 4-km resolution GOES-East satellite IR images of tropical cyclones from the Atlantic basin between 2003 and 2006. The original GOES-E image is reduced to a 480x640 pixel image centered on the tropical cyclone. Best track data for each tropical cyclone from HURDAT (http://www.nhc.noaa.gov/tracks1851to2008_atl_reanal.txt) is used to center the images, and after the best track data ends, the centers are found using a combination of locations from Kofron et. al. (2009a) and manual calibration. TC intensities (maximum winds and minimum central pressure) are included with HURDAT, but after the end of the best track data, the maximum winds are found using 1° resolution NCEP FNL re-analyses.

The DAV-T uses a signal variance calculated directly from satellite infrared brightness temperature images (Piñeros et al. 2008). First, a gaussian blur is applied to each pixel in the image in order to alleviate some of the sharpness in the image. The gradients of the blurred brightness temperatures are then calculated by applying a Sobel template (Bow 2002) at every pixel. Each pixel then has an associated gradient direction that can be compared to an ideal vortex (Figure 1a), which has all gradient directions aligned along radials toward the center or away from the center (Figure 1b). Using each pixel in the original image in turn as the center of reference, the difference between the brightness temperature gradient direction and a radial extending from that reference center is calculated for every pixel within 350 km of the reference center (e.g., Fig. 1b). A histogram of the deviation angles is built and the variance of the deviation angles (DAV) in that histogram is calculated. The resulting DAV value is a single numerical value for the “organization” of the TC surrounding that location (Piñeros et. al. 2008).

For this study, the above is applied to each resized and centered image for an area of 141 by 141 pixels (or 564 by 564 km) around the center of the image. If the brightness value at the individual pixel does not exceed some threshold value (0.11 for this study), the DAV is

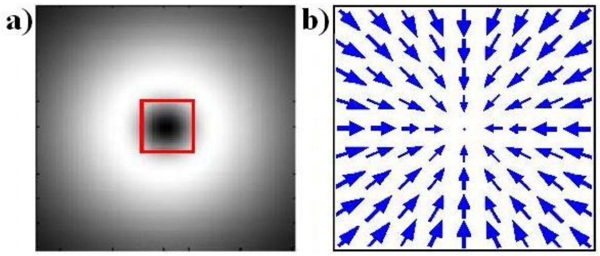

Figure 1: a) Vortex of an ideal and perfectly symmetric TC and b) the gradient matrix of the ideal and perfectly symmetric TC vortex (from Piñeros et al. 2008).

not calculated for that pixel. Both the absolute minimum DAV value and an average DAV value are extracted from the image so that one value can be used to represent the symmetry of the cyclone. The average DAV is calculated for a 101 by 101 pixel box centered on the image center. For each DAV value, a 6-hour running mean is applied in order to reduce the noise of the data.

TCs are chosen from the Atlantic hurricane basin that satisfy several different patterns of recurvature into the mid-latitudes. The patterns include ET of a TC that interacts with an upstream trough and reintensifies as either a cold-core cyclone (Hurricane Florence 2006) or through warm-seclusion processes (Hurricane Irene 2005), a TC that interacts with a downstream trough and reintensifies, a TC that dissipates post-transition (Hurricane Charley 2004), and a TC that recurves but does not undergo ET (Tropical Storm Bill 2003) (Kofron et. al. 2009a, 2009b). ET from a downstream trough interaction with reintensification is not represented because of significant missing data from the satellite imagery dataset.

3. SUMMARY

3.1 *Cold-core Upstream Trough ET – Hurricane Florence*

Hurricane Florence began as an easterly tropical wave that propagated off of the west coast of Africa. At 06 UTC on September 5th, 2006 the intensity was upgraded to tropical storm strength. Figure 2a shows that the DAV values associated with the center of the storm were rather high and that the wave was elongated from the southwest to the northeast. Over time, the storm became more organized (Figure 2b) and intensified to hurricane strength at 06 UTC on the 10th of September. However, the minimum DAV in Figure 2b was low and collocated with the true center of the cyclone, which indicates that the storm was well organized. Florence reached peak intensity of 80 kt and a minimum central pressure of 975 mb at 00 UTC on the 11th but had clearly begun to interact with the mid-

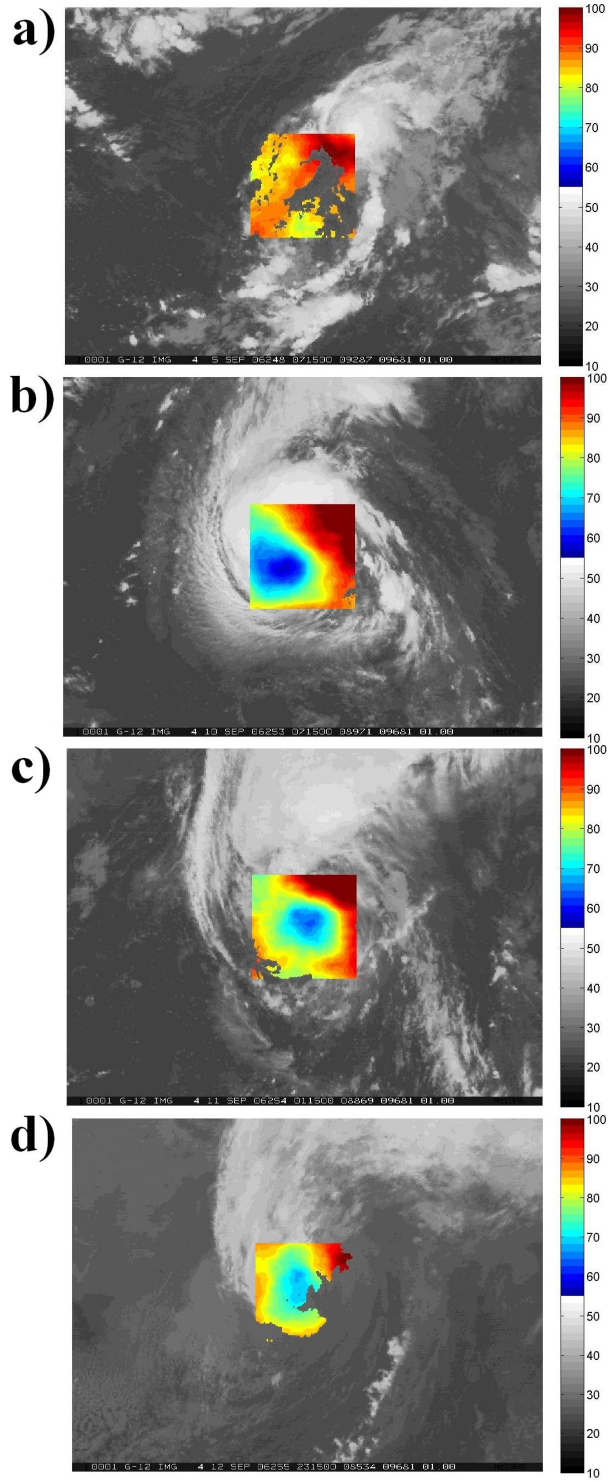

Figure 2: 480 by 640 pixel (4 km resolution) IR satllite images with DAV values (divided by 30 for scaling purposes) at the center for Hurricane Florence when the TC was a) a tropical storm on September 5th, 2006 at 06 UTC, b) a hurricane on September 10th, 2006 at 06 UTC, c) at maximum intensity on September 11th, 2006 at 00 UTC, and d) extratropical on September 13th, 2006 at 00 UTC.

latitude environment (Figure 2c). The minimum DAV was still low and collocated with the center of the TC, but the IR imagery outside of the DAV box in Figure 2c shows that a large field of high clouds extends poleward of the TC. Finally, on the 13th at 00 UTC, Florence was declared extratropical (the ET time) with hurricane strength winds at 70 kt and a minimum central pressure of 978 mb. At this time, dry air began to dominate the TC, especially on the east side of the circulation (Figure 2d), and the DAV values generally increased. Within 18 hours, the minimum central pressure dropped 15 mb to 963 mb and the maximum wind remains at 70 kt.

According to the Klein et. al. 2001 subjective criteria for the transformation stage, Florence began transition much earlier than when it was declared extratropical. So, it is likely that the time that Florence was declared extratropical was the completion of the transformation stage, and the drop in pressure during the 18 hours after being declared extratropical was the reintensification stage. However, it is not clear at what time the circulation became embedded in the mid-latitude baroclinic zone, which would indicate the end of the transformation stage of ET. Figure 3 for the DAV values shows a large increase, especially for the average DAV, between 00 UTC and 12 UTC on September 12th, which could indicate the ET time. Although it is 18 hours prior to the time that Florence was declared extratropical, the TC clearly became more asymmetric. In addition, the DAV values decrease dramatically near the end of the reintensification.

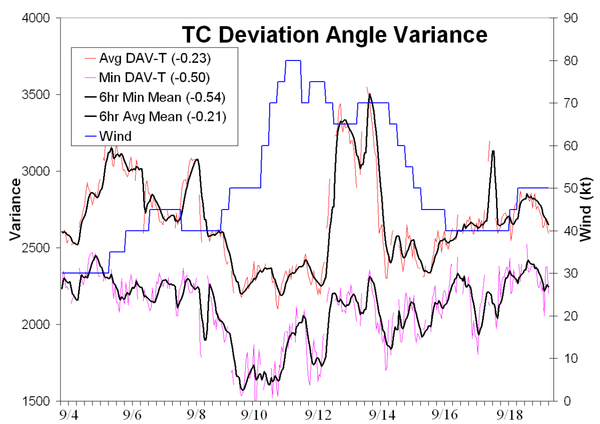

Figure 3: Plots of the average DAV (upper black line) and the absolute DAV (lower black line) values as a 6-hr running mean versus wind (blue line). The orange and purple lines are the hourly DAV values, respectively. The values in parentheses are the correlation coefficients of that variable with wind speed.

3.2 *Warm-seclusion Upstream Trough ET – Hurricane Irene*

Hurricane Irene also began as an easterly tropical wave that propagated off of the west coast of Africa. As a wave, it quickly traversed away from the warmest waters in the ITCZ and struggled to maintain itself. Irene was first named a tropical storm on the 7th of August 2005 at 12 UTC but was downgraded again to tropical depression shortly thereafter. On August 11th at

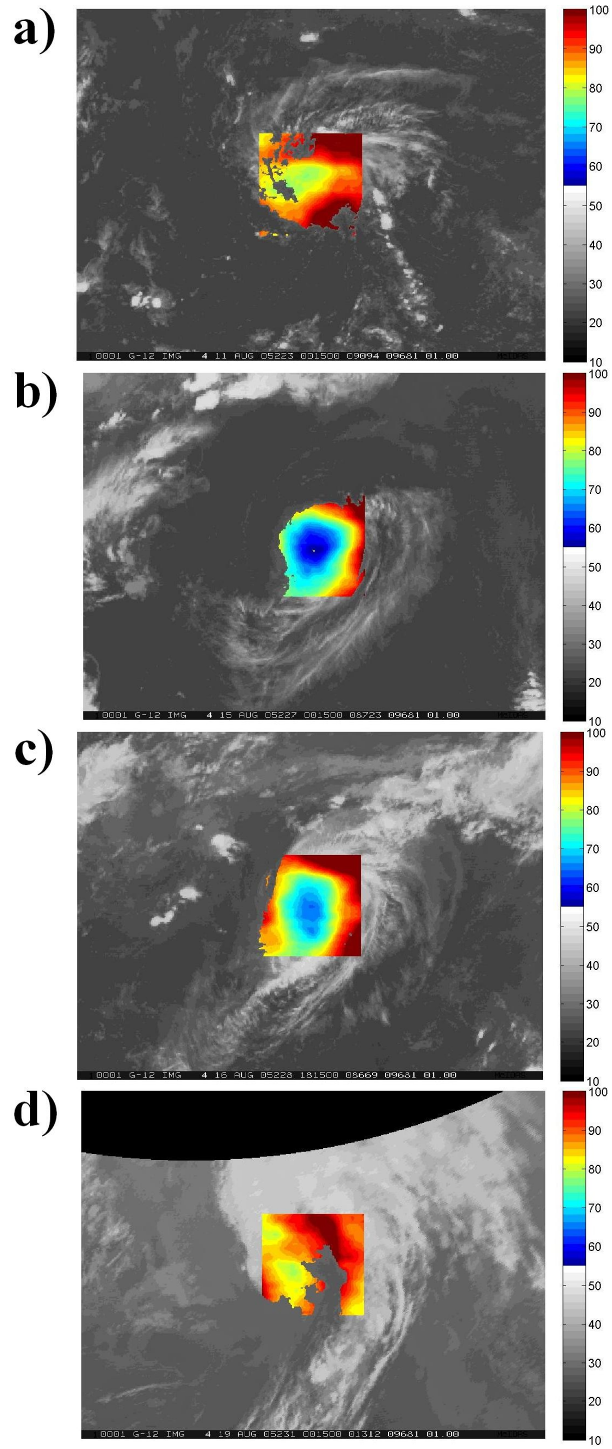

Figure 4: As in Figure 2 for Hurricane Irene when the TC was a) a tropical storm on August 11th, 2005 at 6Z, b) a hurricane on August 15th, 2005 at 6Z, c) at maximum intensity on August 16th, 2005 at 18Z, and d) extratropical on August 19th, 2005 at 0Z.

00 UTC, Irene was again upgraded to tropical storm intensity, and, although it was a relatively small storm, DAV values for several days and began to recurve prior to becoming a hurricane on August 15th at 00 UTC at

the DAV values were relatively low near the TC center (Figure 4a). Irene remained a tropical storm with low which time Hurricane Irene was a small but concentric TC with very low DAV values (Figure 4b). At 18 UTC on the 16th, Irene reached maximum intensity with winds of 90 kt and a minimum central pressure of 970 mb. Between the maximum intensity time and the time that Irene first reached hurricane strength, it appears that the TC underwent some changes in which it became slightly disorganized and elongated before reorganizing and becoming symmetric again at the maximum intensity (Figure 4c). However, at this time it also appears that the northern periphery of Irene was beginning to interact with the mid-latitude environment, which again caused some elongation of the cloud structure. By August 18th at 12 UTC, the remains of Irene were interacting strongly with a mid-latitude trough and the circulation center remained in between the trough to the west and the remaining central dense overcast associated with Irene. After this time, the best track did not register Irene as an extratropical transition; however, because the remnants of Irene likely contributed in coordination with mid-latitude processes, it is included as an ET case. Only 12 hours later, the combination of the trough and remains of Irene began to look much like a classical mid-latitude extratropical cyclone with a large area or warm-frontal-like cloud structure to the north and a cold-frontal-like area extending to the south (Figure 4d). Kofron et. al. (2009a) found that this storm was a warm-seclusion ET case from examination of Hart's cyclone phase-space (Hart 2003). Over time, the extratropical cyclone became mature and occluded and the DAV values decreased until the cyclone began to decay, at which time the DAV values increased again (Figure 5).

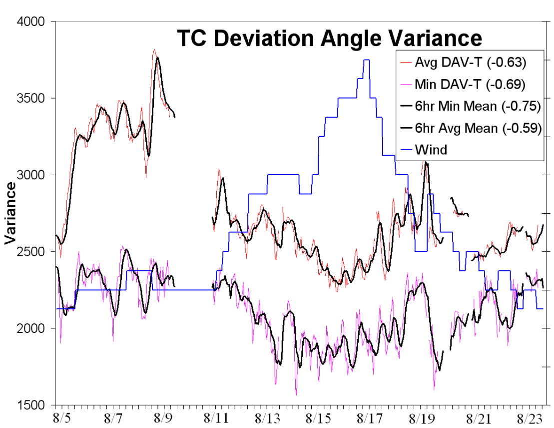

Figure 5: As in Figure 3 for Hurricane Irene.

Although there is no large spike as for Hurricane Florence, there is a significant rise in the DAV as Irene began to interact more strongly with the mid-latitude trough (Figure 5). However, similar to Florence, the absolute maximum DAV coincides with a restrengthening of the winds after reaching maximum intensity. That means that there may be some potential for assigning threshold values using DAV for the ET time and the ET completion time.

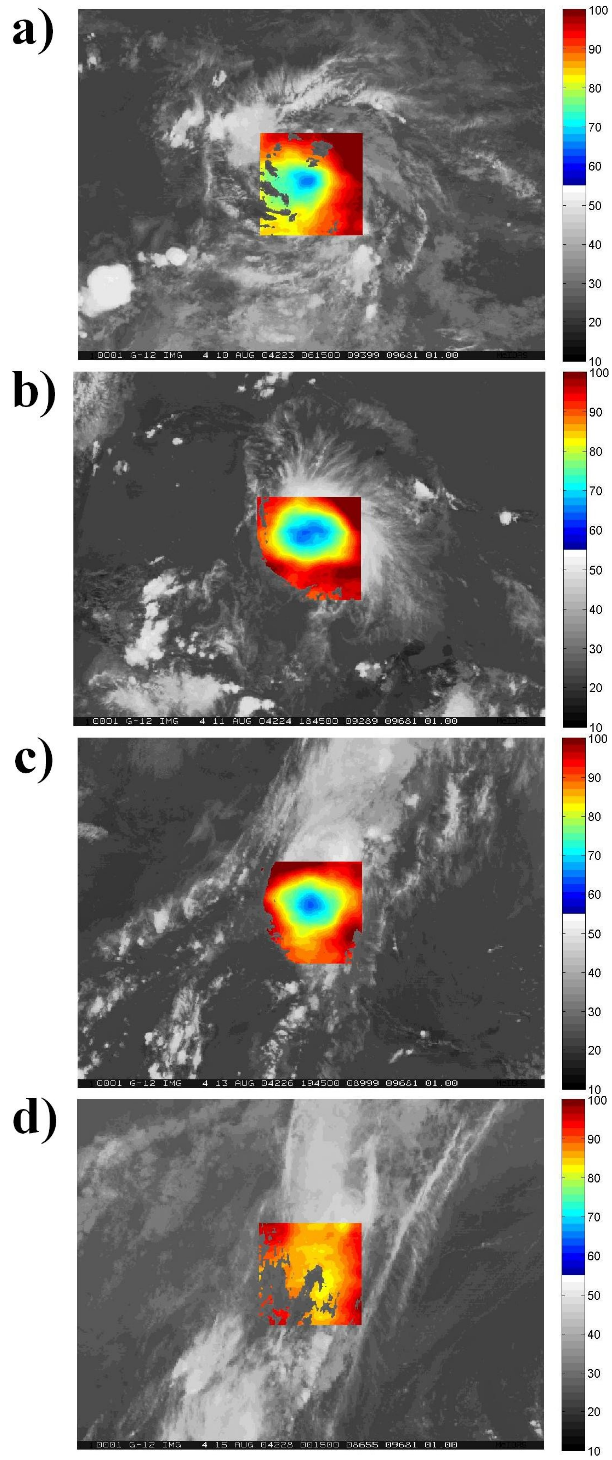

Figure 6: As in Figure 2 for Hurricane Charley when the TC was a) a tropical storm on August 9th, 2004 at 12Z, b) a hurricane on August 11th, 2004 at 18Z, c) at maximum intensity on August 13th, 2004 at 19Z, and d) extratropical on August 15th, 2004 at 0Z.

3.3 *Post-transition Dissipation – Hurricane Charley*

Charley became a tropical depression just before entering the Caribbean Sea on August 9th, 2004 at 12

UTC. In less than 24 hours, Charley was named a tropical storm with a small but rather symmetric center (Figure 6a). After only another 36 hours at a location just to the south of Jamaica, Charley became a hurricane on August 11th at 18 UTC. The TC remained relatively small and still very symmetric with low DAV values at the center (Figure 6b). Just before landfall at 19 UTC on the 13th of August, Charley reached maximum intensity with maximum winds at 130 kt and a minimum central pressure of 941 mb. At this time, the TC had already begun its recurvature and its interaction with a mid-latitude trough on the northwest side of the storm. The DAV values remained low but confined to a small area at the very center of the storm (Figure 6c). By 00 UTC on August 15th, Charley's circulation center was embedded in the baroclinic zone associated with the mid-latitude trough. It is at this time that Charley was declared extratropical in the best track data. The actual center lost any of the high cloud tops and the DAV values rose dramatically (Figure 6d).

The time series plot of DAV values in Figure 7 show the progression of symmetry of Hurricane Charley. Because the TC was generally symmetric throughout its tropical life, the DAV values remained relatively constant until the interaction with the trough began just after landfall on the 14th of August. Throughout the ET lifecycle, the DAV values continue to rise. This is consistent with the finding from Kofron et. al. (2009a and 2009b) that Charley dissipates post-transition.

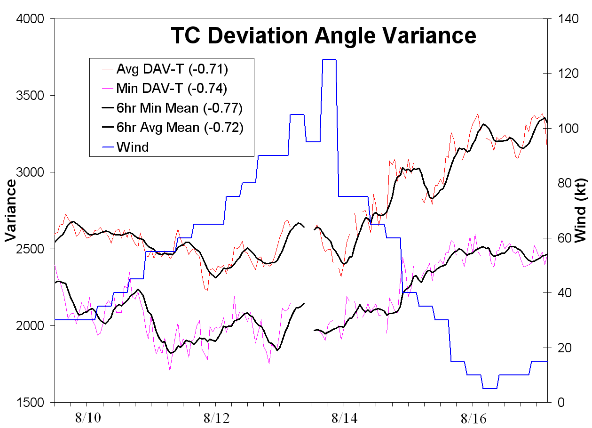

Figure 7: As in Figure 3 for Hurricane Charley.

3.4 *Recurving Non-ET – Tropical Storm Bill*

The final storm in this study is Tropical Storm Bill from 2003. This storm began as a low that cut off from a mid-latitude trough over the Yucatan Peninsula. Soon after emerging into the Gulf of Mexico, it was upgraded to a tropical depression and soon after to a tropical storm on June 29th, 2003 at 12 UTC. It is clear from Figure 8a that the majority of thunderstorm activity was displaced north and east of the center of circulation and the DAV values near the center were low. Also, it looks as though the trough that Bill developed from was still affecting the storm on the north side. By the 30th at 18 UTC, the trough had less of an effect on the circulation of Bill (Figure 8b) and the storm was allowed to intensify

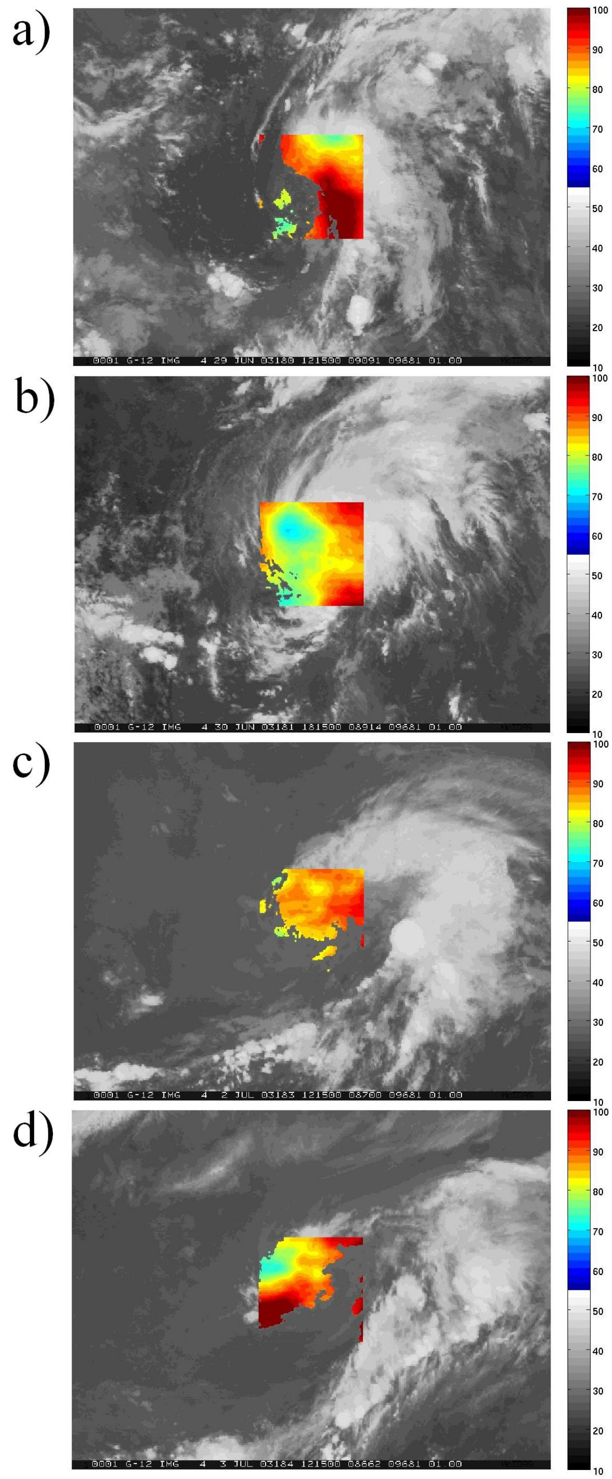

Figure 6: As in Figure 2 for Tropical Storm Bill when the TC was a) a tropical storm on June 29th, 2003 at 12Z, b) at maximum intensity on June 30th, 2003 at 18Z, c) just before being declared ET on July 2nd, 2003 at 12Z, and d) as a dissipating low on July 3rd, 2003 at 12Z.

over the warm waters of the Gulf of Mexico just prior to making landfall at 19 UTC. The maximum intensity of 50 reached at 18 UTC on June 30th, and the storm already began to recurve to the northeast. The DAV values near the center decreased and the storm was generally more kt winds and 997 mb minimum central pressure was symmetric. After making landfall in eastern Louisiana, Bill quickly weakened back to tropical depression strength and accelerated to the northeast on the back end of the mid-latitude trough. Strangely, the storm became more symmetric over land and the DAV values continued to drop (not shown). Just before being declared extratropical at 12 UTC on July 2nd, Bill took on a shape similar to an extratropical cyclone (Figure 8c) with high DAV values around the circulation center. At that time, it appears that Bill was undergoing ET. However, 24 hours later at 12 UTC on the 3rd of July, the circulation center looked to be detaching itself from the trough (Figure 8d). The circulation center stalled and dissipated; therefore, Bill is considered a non-ET case.

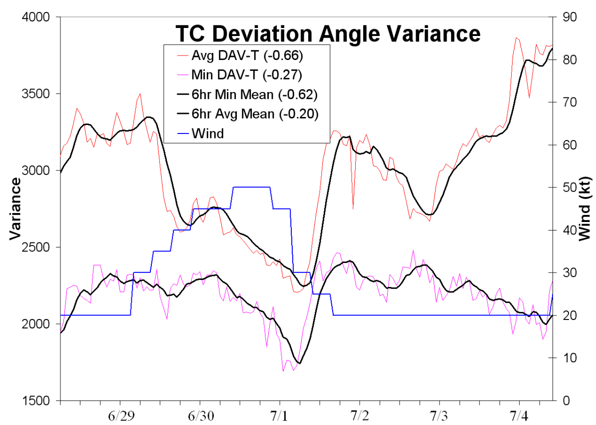

Figure 9: As in Figure 3 for Tropical Storm Bill.

Because Bill did not surpass tropical storm strength, the DAV values were relatively high for the whole time series. However, they do lower during the brief period that Bill was at moderate tropical storm strength. After significant weakening of the maximum winds, the DAV values increased sharply, which indicates a significant loss of symmetry. This conforms with the expectations because of the interaction with the mid-latitude trough from Figure 6b to 6c, but the DAV values decreased as the circulation center began to detach from the trough later on July 2nd. The DAV values again rose as Bill dissipated, but it is not clear why the values decreased before dissipation.

4. CONCLUSIONS AND FUTURE WORK

Although the research is in its early stages, there appear to be several aspects of the DAV-T that may work for the ET of TCs. The TCs that interact with an upstream trough and reintensify (Hurricane Florence and Hurricane Irene) clearly show a dramatic rise and fall of the DAV values, which may coincide with the transformation period and reintensification period, respectively. The DAV values for the post-transition dissipation TC (Hurricane Charley) have a slower and much steadier rise throughout the time series until the remnants of the circulation center are no longer discernible, which is potentially indicative of the beginning of the transformation stage but not the end. Finally, the recurving TC that does not undergo ET (Tropical Storm Bill) shows a similar DAV pattern as the post-transition reintensification TCs with a significant rise in values as the storm weakens and a brief decrease in the DAV values as the circulation center disengages the mid-latitude trough. However, there is no change in the maximum winds, so the decrease does not coincide with a period of intensification. In all, there appear to be patterns potentially associated with the different aspects of the ET or the non-ET of TCs.

Future work will include an attempt at establishing critical threshold values for determining the ET time and the ET completion time, which may coincide with the reintensification period for the post-transition reintensification ET cases. In addition, different IR channels will be examined in order to determine if shorter wavelength satellite imagery can detect the circulation center with more ease than the IR used in this study.

Acknowledgements This work has been supported by the National Science Foundation under grant ATM-0730079.

5. REFERENCES

Bow, S. T., 2002: *Pattern Recognition and Image Processing*. New York: Marcel Dekker, 2nd ed., 311-312.

Demirci, O., J. S. Tyo, and E. A. Ritchie, 2007: Spatial and spatiotemporal projection pursuit techniques to predict the extratropical transition of tropical cyclones. *IEEE Trans. Geo. Remote Sensing*, **45**, 418-425.

Evans, J. L., and R. E. Hart, 2003: Objective indicators of the life cycle evolution of extratropical transition for Atlantic tropical cyclones. *Mon. Wea. Rev.*, **131**, 909-925.

Harr, P. A., and R. L. Elsberry, 2000a: Extratropical transition of tropical cyclones over the western north Pacific. Part I: Evolution of structural characteristics during the transition process. *Mon. Wea. Rev.*, **128**, 2613-2633.

Hart, R. E., 2003: A cyclone phase space derived from thermal wind and thermal asymmetry. *Mon. Wea. Rev.*, **131**, 585-616.

Jones, S. C., P. A. Harr, J. Abraham, L. F. Bosart, P. J. Bowyer, J. L. Evans, D. E. Hanley, B. N. Hanstrum, R. E. Hart, F. Lalaurette, M. R. Sinclair, R. K. Smith, and C. Thorncroft, 2003: The extratropical transition of tropical cyclones: Forecast challenges, current understanding, and future directions. *Wea. Forecasting*, **18**, 1052-1092.

Klein, P. M., P. A. Harr, and R. L. Elsberry, 2000: Extratropical transition of western north Pacific tropical cyclones: An overview and conceptual model of the transformation stage. *Wea. Forecasting*, **15**, 373-395.

Kofron, D. E., E. A. Ritchie, J. S. Tyo, 2009a: Determination of a Consistent Time for the Extratropical Transition of Tropical Cyclones Part I:

Examination of Previous Methods for Defining "ET Time." *Submitted to Mon. Wea. Rev.*

Kofron, D. E., E. A. Ritchie, J. S. Tyo, 2009b: Determination of a Consistent Time for the Extratropical Transition of Tropical Cyclones Part II: Potential Vorticity Metric. *Submitted to Mon. Wea. Rev.*

Piñeros, M. F., E. A. Ritchie, and J. S. Tyo, 2008: Objective Measures of Tropical Cyclone Structure and Intensity Change from Remotely Sensed Infrared Image Data. *IEEE Trans. Geo. Remote Sensing*, **46**, 3574-3580.